ACS APPLIED MATERIALS & INTERFACES

www.acsami.org

Research Article

Developing Highly Tough, Heat-Resistant Blend Thermosets Based on Silicon-Containing Arylacetylene: A Material Genome Approach

Guanru Gao,[#] Songqi Zhang,[#] Liquan Wang,* Jiaping Lin,* Huimin Qi, Junli Zhu, Lei Du, and Ming Chu

Cite This: *ACS Appl. Mater. Interfaces* 2020, 12, 27587−27597

Read Online

ACCESS | Metrics & More | Article Recommendations | Supporting Information

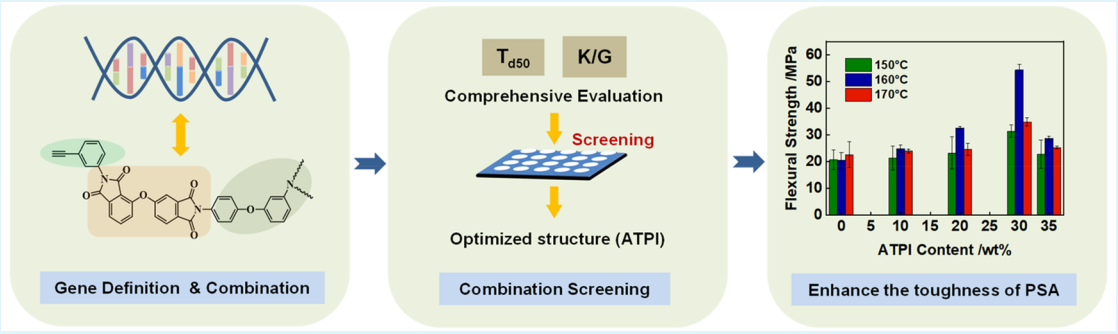

ABSTRACT: Silicon-containing arylacetylene (PSA) resins exhibit excellent heat resistance, yet their brittleness limits the applications. We proposed using acetylene-terminated polyimides (ATPI) as an additive to enhance the toughness of the PSA resins and maintain excellent heat resistance. A material genome approach (MGA) was first established for designing and screening the acetylene-terminated polyimides, and a polyimide named ATPI was filtered out by using this MGA. The ATPI was synthesized and blended with PSA resins to improve the toughness of the thermosets. Influences of the added ATPI contents and prepolymerization temperature on the properties were examined. The result shows that the blend resin can resist high temperature and bear excellent mechanical properties. The molecular dynamics simulations were carried out to understand the mechanism behind the improvement of toughness. The present work provides a method for the rapid design and screening of high-performance polymeric materials.

KEYWORDS: *material genome approach, silicon-containing arylacetylene, polyimide, toughness, heat resistance*

1. INTRODUCTION

Silicon-containing arylacetylene (PSA) resins can be used as the matrixes of advanced polymer composites because of their excellent performance, such as no curing volatiles, high decomposition temperature, and high char yield after pyrolysis.[1−4] Itoh et al. synthesized the first kind of PSA, poly[(phenylsilylene)ethynylene-1,3-phenyleneethynylene] (abbreviated MSP in their work).[5] They found that these resins are highly heat-resistant, nonflammable, and moldable, which have a 5% decomposition temperature (T_{d5}) of 860 °C and the residue at 1000 °C of 94%. The PSA, however, is brittle, which becomes the bottleneck in improving the performance of the materials.[6] Improving the toughness is crucial for the engineering applications of the PSA resins.

Various methods have been developed to improve the toughness of the PSA resins. One of the approaches is the synthesis of novel molecules with flexible groups in their main chain, but it usually causes a dramatic reduction of the heat resistance of the resins.[7] Alternatively, syntheses of copolymers or preparations of polymer blends are effective ways to toughen the PSA resins. For example, the PSA resins were modified by dipropargyl ether from melt blending or blended with benzoxazines to improve the toughness.[8,9] Despite a series of attempts, there is still a gap from the expected performance—either the thermal stability is significantly decreased or the toughness is not sufficiently improved. Polyimide, especially thermosetting polyimide capped by reactive end groups, shows excellent comprehensive properties such as pretty good thermal stability, high toughness, and strong adhesion with reinforced fibers.[10−14] Compared to the PSA resins, the polyimides exhibit lower thermal stability but better mechanical properties. Because the PSA resins contain alkynyl groups,[15−17] the acetylene-terminated polyimide can be selected as a blend to toughen PSA resins via the reaction of the terminal alkynyl groups of two resins during the curing

Received: April 6, 2020
Accepted: May 27, 2020
Published: May 27, 2020

Downloaded via EAST CHINA UNIV SCIENCE & TECHLGY on October 23, 2020 at 12:11:48 (UTC).
See https://pubs.acs.org/sharingguidelines for options on how to legitimately share published articles.

© 2020 American Chemical Society

https://dx.doi.org/10.1021/acsami.0c06292
ACS Appl. Mater. Interfaces 2020, 12, 27587−27597

process. However, it is challenging to choose an effective acetylene-terminated polyimide that can enhance the toughness of the PSA resins without substantially sacrificing the heat resistance.

Traditionally, the experimental trial-and-error method is used to find polyimides that can effectively toughen the PSA resins. The traditional method, however, has led to a long research cycle, low efficiency, and severe resource consumption because of the wide variety of polyimides. It is also difficult to obtain optimized polymers through such a trial-and-error method. For example, it took two decades to explore and exploit thermally stable LaRC polyimides step-by-step from a multitude of polymer structures and compositions.[18] The materials genome approach (MGA), which aims at accelerating the research and development of new materials via combining computation, database searches, and experiments, renders it possible to solve this problem.[19−23] The MGA has successfully been used in the screening of energy-containing materials, high-temperature alloys, and inorganic porous materials.[24−27] The MGA can also apply to the design of polymers.[28−32] For example, Ramprasad et al. established a rational design strategy of hierarchical modeling with successive down-selection stages to accelerate the discovery of advanced polymer dielectrics for capacitive energy storage applications.[29] In the MGA for polymers, the atoms or chemical groups can be regarded as genes. These genes can be combined through covalent bonds to generate candidate polymers with a series of chemical sequences. Different gene types and gene combinations can lead to different properties of the polymers. With the help of efficient theoretical prediction tools for properties, high-throughput screening can be performed before experimental preparation, and therefore, the discovery of optimized polymers among the vast number of candidate polymers could be accelerated.[22]

In this work, we first established an MGA for screening the acetylene-terminated polyimides. An acetylene-terminated polyimide, named ATPI, was filtered out by using the MGA. We then synthesized the ATPI and used them as an additive to enhance the toughness of PSA resins. The mechanical and thermal properties of the PSA resins blended with various contents of ATPI were investigated. It was found that the mechanical properties of the cured blending resins were significantly improved as compared to those of the neat PSA resins, whereas the cured blending resins maintain excellent heat resistance. This work presents a new method for accelerating the research and development of new high-performance resins.

2. METHODS

2.1. Theory and Simulation. *2.1.1. Molecular Connectivity Index.* The molecular connectivity index (MCI) method, based on chemical graph theory, plays a vital role in building the structure−performance relationship of compounds.[33,34] This method, which has been automated by implementing a simple interactive computer program (SYNTHIA), was found to be able to predict the properties of polymers accurately and reliably. In this work, the molecular connectivity index method was used to calculate the 50% decomposition temperature (T_{d50}), bulk modulus (K), and shear modulus (G) of each polymer. The T_{d50} is given by

$$T_{d50} \approx \frac{Y_{d50}}{M} \tag{1}$$

$$Y_{d50} \approx 6.5N + 0.99({}^{1}\chi^{\nu} + N_{Yd} - N_{H}) \tag{2}$$

where N is the number of non-hydrogen atoms in the repeating unit of each polymer and ${}^{1}\chi^{\nu}$ is the first-order connection index determined by the overall molecular configuration. N_{Yd} and N_{H} are the correction terms, and M is the molecular weight of the repeating unit of the polymer.

The bulk modulus K and the shear modulus G are given by[33]

$$K(T) \approx \rho(T)\left[\frac{U_R}{V(T)}\right]^6 \tag{3}$$

$$G(T) \approx \rho(T)\left[\frac{U_H}{V(T)}\right]^6 \tag{4}$$

Here, T is the temperature, ρ is the density of the polymer, and V is the velocity of acoustic waves. U_R is the molar ratio function that is independent of the temperature, and U_H is the molar Hartmann function.

2.1.2. Molecular Dynamics Simulation. We employed the molecular dynamics (MD) simulation method to study the phase behavior of the blend resins. MD is a powerful and versatile simulation method that allows one to predict the equilibrium and transport properties of classical many-body systems.[35−37] The MD simulation was implemented in Materials Studio.[38] In the present simulation, 20 ATPI with a degree of polymerization of 1, 89 PSA with a degree of polymerization of 2, and 1267 *N*,*N*-dimethylformamide (DMF) molecules are randomly mixed in a cubic box with periodic conditions, which is relaxed in the NPT ensemble at the temperature of 23 °C (300 K) for 60 ps. In this blend, the weight ratio of ATPI to PSA is 3:7, and the ATPI content is 12.4 wt %. The interactions between atoms are described by the COMPASS force field, which is an *ab initio* force field. To study the phase behavior, we performed the MD simulations in the NPT ensemble at the temperature of 140, 150, 160, 170, and 180 °C for 200 ps, respectively. Detailed descriptions of the methods can be found in section 1 of the Supporting Information.

2.2. Experimental Section. *2.2.1. Preparation and Curing of ATPI.* 3,4′-Oxidiphthalic anhydride (ODPA) (21.4 g, 0.069 mol) and DMF (130 mL) were first put into a flame-dried 500 mL three-necked round-bottom flask equipped with a nitrogen inlet, magnetic stirrer, and drying tube. Then 3,4-oxidianiline (ODA) (9.21 g, 0.046 mol), dissolved in 70 mL of DMF, was added to the flask. The reaction mixture was stirred in a nitrogen atmosphere at room temperature for 2 h. Afterward, 3-ethynylaniline (APA) (5.39 g, 0.046 mol), dissolved in 24 mL of DMF, was added. The mixture was stirred at room temperature for 4 h. Acetic anhydride (14.09 g, 0.138 mol) and triethylamine (13.96 g, 0.138 mol) were added in turn with stirring for 12 hours. Subsequently, a large excess of ethanol was added to the solution. The precipitate was collected by filtration and washed thoroughly with ethanol four times. The product was dried under vacuum at 50 °C for several hours, and a gray powder was finally obtained.

2.2.2. Preparation and Curing of PSA/ATPI Blend Resins. The PSA/ATPI blends with various contents of ATPI were first added into a 250 mL single-neck eggplant flask, and then DMF was added. A homogeneous solution was obtained after the two resins were entirely dissolved. The solution was then prepolymerized at 150, 160, and 170 °C for 1 h, respectively. After prepolymerization, the DMF was removed by reduced pressure distillation. Finally, a homogeneous viscous resin was obtained. This resin was poured into a mold and placed into a vacuum oven at 100 °C. After 1−2 h, the resin was moved into another oven under air and cured at 150 °C for 4 h, 210 °C for 2 h, 240 °C for 2 h, and 260 °C for 2 h.

2.2.3. Characterizations of ATPI and PSA/ATPI Blend Resins. Both the molecular structure of the ATPI and the thermal curing behavior of the PSA/ATPI resin were characterized by a Fourier transform infrared spectrometer (FTIR, Nicolet 6700, Thermo Electron). In addition to FTIR, the molecular structure of the ATPI was characterized by proton nuclear magnetic resonance (^{1}H NMR, Avance 400, Bruker). The flexural properties of cured PSA/

https://dx.doi.org/10.1021/acsami.0c06292
ACS Appl. Mater. Interfaces 2020, 12, 27587−27597

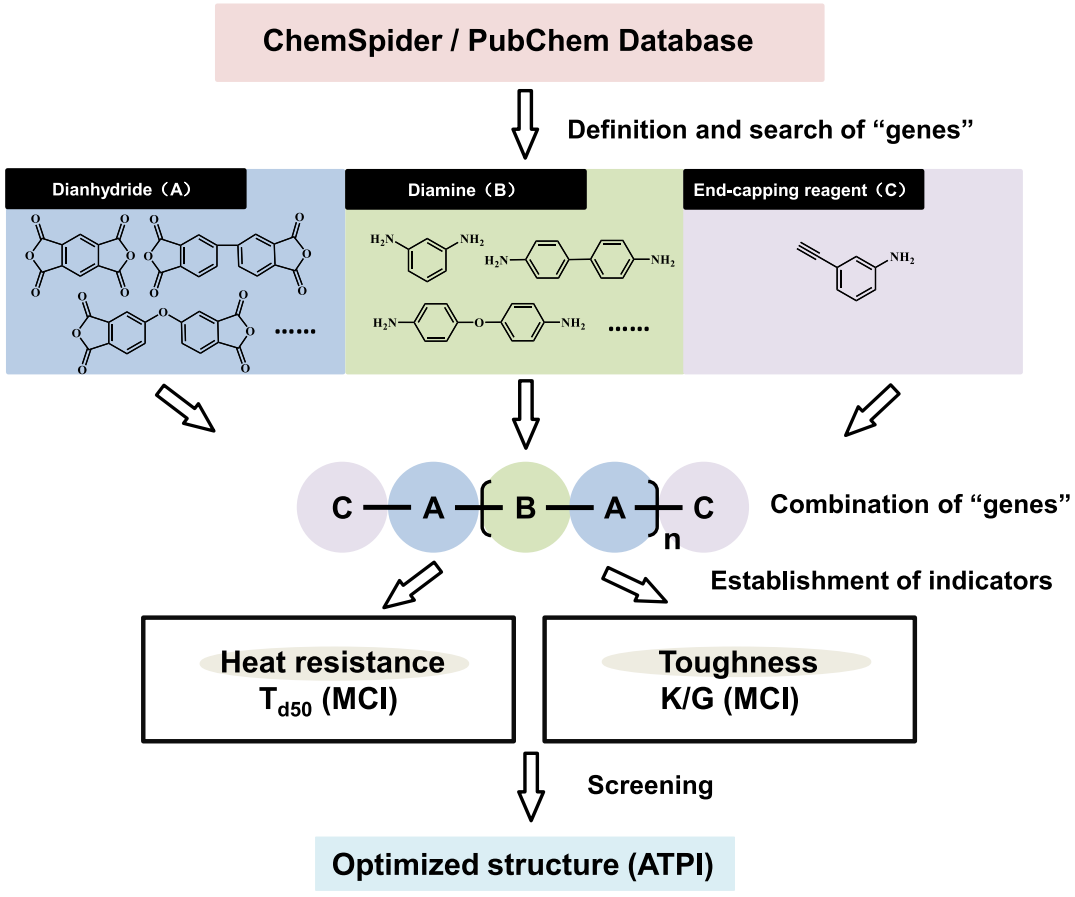

Figure 1. Procedures developed for the design and rapid screening of ATPI. Herein, the dianhydride monomer, diamine monomer, and end-capping reagents are defined as the **A**, **B**, and **C** genes. The T_{d50} and K/G are calculated by the molecular connectivity index (MCI).

ATPI resins were measured with an electronic universal testing machine (CMT 4204, New Sansi Material Testing Co., Ltd.). The fracture surface morphologies of cured PSA/ATPI resins were observed with a scanning electron microscope (SEM, S4800, Hitachi). The heat resistance of cured ATPI and PSA/ATPI resins were examined by thermogravimetric analyses (TGA, TG209F1, NETZSCH). The rheological properties of PSA/ATPI resins were obtained by the rotary rheometer (MCR 302, Anton Paar). The chemical structure of the cured PSA/ATPI resin was analyzed by gas chromatography-mass spectrometry (GC-MS, 7890A-5975C, Agilent). The detailed experimental information is presented in section 2.2 of the Supporting Information.

3. RESULTS AND DISCUSSION

We first established a materials genome approach (MGA) for screening acetylene-terminated polyimides that bear high thermal stability and high toughness. Then an acetylene-terminated polyimide, named ATPI, was filtered out and synthesized. The obtained ATPI was blended with the PSA resin to enhance the toughness of the PSA resin without losing much thermal stability.

3.1. Materials Genome Approach for Screening Acetylene-Terminated Polyimides. Figure 1 shows the MGA developed for the design and rapid screening of acetylene-terminated polyimides. As shown, the MGA contains three main steps, that is, definition and acquisition of genes, gene combination, and screening. As far as we know, the nucleotides in DNA or RNA are genes that determine the genetic characteristics of living organisms.[39] The types and sequence of nucleotides constitute various genetic characteristics. We introduced the concept of "genes" in biology to the resin system for designing and screening acetylene-terminated polyimides. In principle, the choice of the gene can be either atoms or chemical groups. For the sake of synthesis, we defined the chemical groups as the "genes" of the polymers. Because the acetylene-terminated polyimides are generally synthesized via the reaction between dianhydride, diamine, and end-capping reagents, we chose the dianhydride monomer, diamine monomer, and end-capping reagents as the **A**, **B**, and **C** genes, respectively. Both the type of the "gene" and the combination of the "gene" can affect the performance of the polymers. Herein, we only focused on the choice of **A** and **B** genes by fixing the **C** gene as 3-ethynylaniline because there is ample space available for the **A** and **B** genes but limited **C** gene for selection. Before the screening, we collected 27 kinds of **A** genes (see Table S1) and 10 types of **B** genes (see Table S2) from the ChemSpider and PubChem databases through a similarity search. In the similarity search, the constraint that the structures of the genes are both difunctional and commercially available was applied. For convenience, the 27 kinds of **A** genes and 10 types of **B** genes were numbered in sequence (for the sequence number, see Tables S1 and S2). Then the **A**, **B**, and **C** genes were combined into a series of polyimide resins in a sequence that we designed, and as a result, 270 kinds of designed resins are generated.

In what follows, we continued to screen the optimized resins from the 270 combination structures. Because we attempted to obtain a structure with both heat resistance and high toughness, the thermal property and the toughness of the

https://dx.doi.org/10.1021/acsami.0c06292
ACS Appl. Mater. Interfaces 2020, 12, 27587−27597

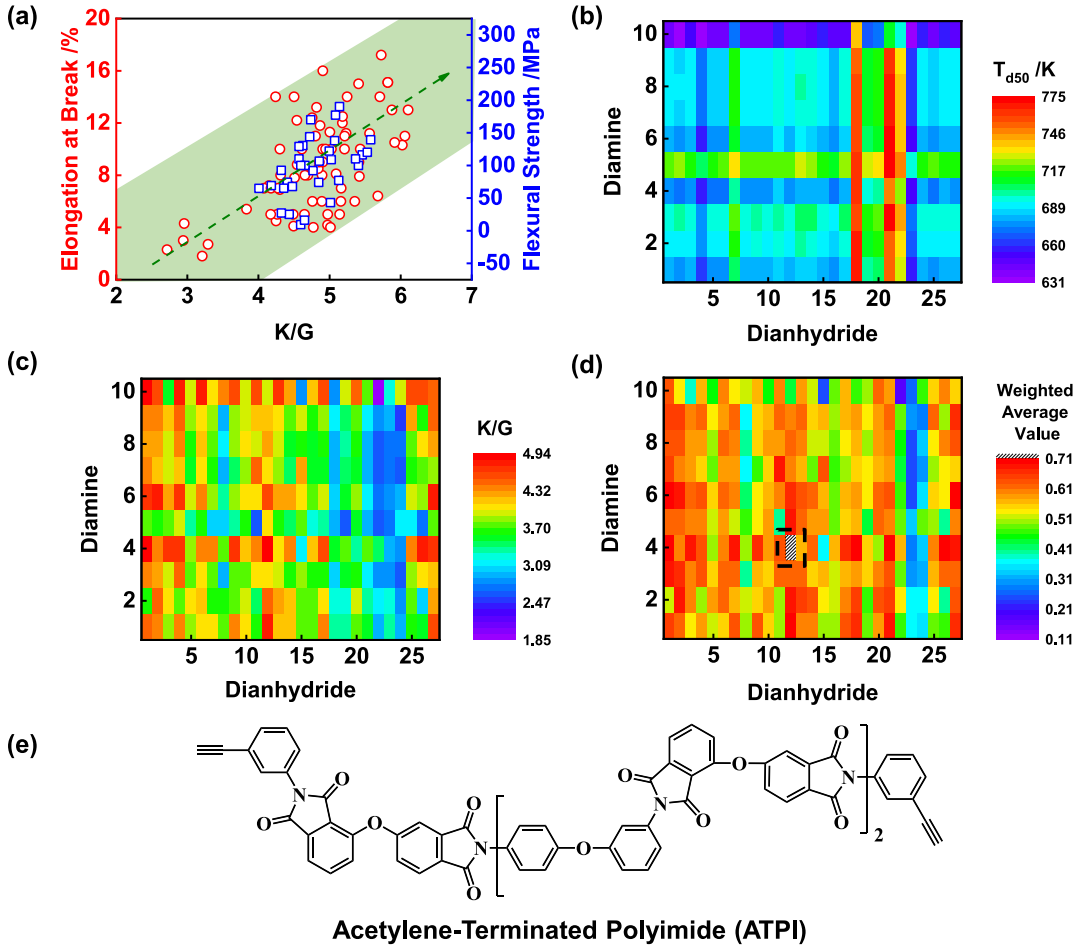

Figure 2. (a) Plots of elongation at break (red circles) and flexural strength (blue squares) against K/G. The data of elongation at break or flexural strength are collected from the PoLyInfo database and the literature listed in section 4 of the Supporting Information. Heat maps of (b) T_{d50} values, (c) K/G values, and (d) weighted-average values for various gene combinations. The colors from purple to red correspond to the values from low to high. In (d), the shadow rectangle circled by a black dotted line represents the screened ATPI. (e) Molecular structure of the screened ATPI.

270 combination structures should be evaluated. Two corresponding indicators were established, that is, 50% decomposition temperature (T_{d50}) representing the level of heat resistance and the ratio of bulk modulus to shear modulus (K/G) representing the level of toughness. The proxy K/G for toughness was extracted from the analysis of the available data. Because the elongation at break and flexural strength are associated with the toughness of the materials, we first collected the elongation at break and flexural strength of a series of polymers from the PoLyInfo database[40] and the literature listed in section 4 of the Supporting Information. We then calculated the K/G of these polymers and plotted the elongation at break (red circles) and flexural strength (blue squares) against K/G. The result is given in Figure 2a. As shown, the elongation at break and flexural strength are closely correlated with the K/G, where the Pearson correlation coefficients are 0.61 and 0.48, respectively. Therefore, the K/G can be considered an indicator for evaluating the toughness of the resins. Generally, the high K/G value can represent the high elongation at break or flexural strength and, thereby, the high toughness of the resins.

Figure 2b,c shows the heat maps for T_{d50} and K/G values of each combination structure, respectively. In each figure, the colors from purple to red correspond to the values from low to high. As shown in Figure 2b, the combination structures consisting of no. 18 or no. 21 dianhydrides have better heat resistance. For the toughness, as shown in Figure 2c, the combination structures consisting of no. 12 dianhydride, no. 4 diamine, or no. 10 diamine bear better toughness in general. Because the dependence of the gene types on different properties is different, from Figure 2b and Figure 2c, it is still unclear which combination structure has both high heat resistance and high toughness. Therefore, a full score of the two indicators of the combination structure is required to obtain the optimized structure.

To obtain the resin with the best comprehensive performance, we established an evaluation method for the selection of the optimized resin. First, we normalized the indicators of T_{d50} and K/G, where the optimized value and the worst value become 1 and 0, respectively, Then we endowed each indicator a weight coefficient in terms of its importance. Considering that the polyimides have better thermal properties and the PSA has much lower toughness, we endowed the K/G with a larger coefficient than T_{d50}. Here, the weight coefficients of K/G and T_{d50} are 0.4 and 0.6, respectively. Note that the screened results are unvaried if we further increase the weight coefficient of K/G to, for example, 0.7. The weighted-average values, representing the comprehensive properties of the materials, were finally obtained for various genetic combinations. Figure 2d shows the heat map of weighted-average values. One can

https://dx.doi.org/10.1021/acsami.0c06292
ACS Appl. Mater. Interfaces 2020, 12, 27587−27597

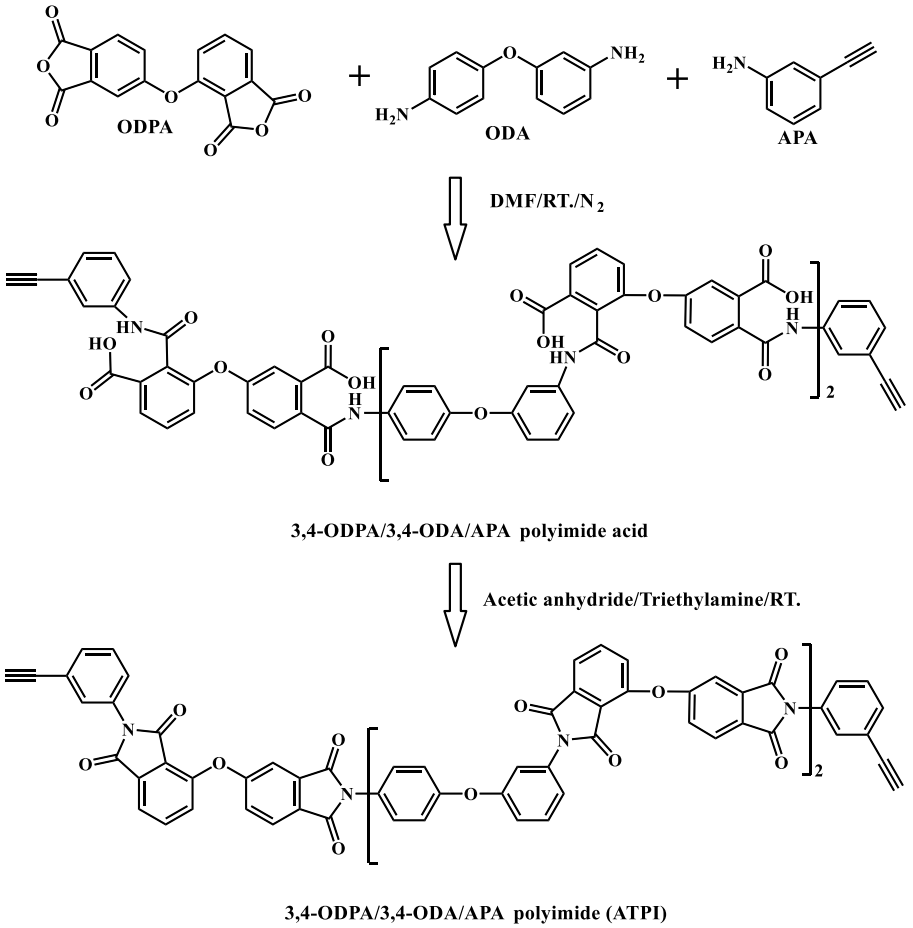

Figure 3. Synthesis routes of the ATPI. ATPI was synthesized by a two-step method with dianhydride monomer (ODPA), diamine monomer (ODA), and end-capping reagent (APA) as raw materials. In the first step, three monomers react to form polyamide acid, and in the second step, the polyamide acid is dehydrated to form polyimide. The number of repeat units of ATPI is 2.

see that the resin from the combination of no. 12 dianhydride and no. 4 diamine, as indicated by the shadow rectangle, exhibits the highest weighted average value (0.7108). We, therefore, selected this resin as the optimized structure and named it as ATPI. The molecular structure of the optimized structure is shown in Figure 2e. Because the solubility of polyimides is crucial for resin processing, we predicted the solubility of the selected ATPI by using a user-friendly online platform named Polymer Genome.[41,42] The prediction result shows that ATPI can dissolve in most common solvents such as DMF, DMAc, and THF (see Table S3). Therefore, the ATPI could have the advantage of easy processing.

We carried out molecular dynamics (MD) simulations to verify the MGA results. Three samples with slightly lower comprehensive scores than ATPI were selected from heat maps and then used as control samples to examine the comprehensive performance of the ATPI. The glass transition temperature and K/G, representing the heat resistance and toughness of the four samples, respectively, were obtained by the MD simulations. The result shows the heat resistance and toughness of the ATPI are higher than those of the other three samples, which verified the results of MGA (for the details, see section 5 of the Supporting Information).

3.2. Preparation of ATPI and Properties of PSA/ATPI Blends. Guided by the screened result from the materials genome approach, we intend to synthesize the ATPI. The synthesis route of ATPI is shown in Figure 3. The ATPI was synthesized by a two-step method with dianhydride monomer (ODPA), diamine monomer (ODA), and end-capping reagent (APA) as raw materials, where the molecular weights can be controlled by adjusting the ratio of reactive monomers and the reaction time. The results of the FTIR spectrum and the ^{1}H NMR spectrum indicate the successful synthesis of ATPI (see section 6 of the Supporting Information). The ^{1}H NMR spectrum indicates that the number of repeat units of ATPI is 2. The solubility of ATPI was also investigated at the experimental level. It was found that the ATPI can dissolve in a series of common solvents, including DMF, DMAc, and THF (for details, see Table S3), which is highly consistent with the results predicted by Ramprasad's methods.

We used the prepared ATPI to blend with PSA to improve the toughness of PSA resins. The PSA/ATPI blend resins were prepared with various contents of ATPI. Because both the ATPI and PSA contain reactive alkynyl groups, they can copolymerize with each other during the prepolymerization and curing process. We analyzed the chemical structure of the cured PSA/ATPI resin by gas chromatography-mass spectrometry (GC-MS). The result shows that the Diels–Alder reaction and radical polymerization reaction mainly occur between the two resins, and the cyclotrimerization reaction also happens during the curing (for details, see section 8 of the Supporting Information). The observation agrees with the results from the density functional theory (DFT) study on the thermal curing mechanism of arylethynyl-containing resins.[43]

https://dx.doi.org/10.1021/acsami.0c06292
ACS Appl. Mater. Interfaces 2020, 12, 27587−27597

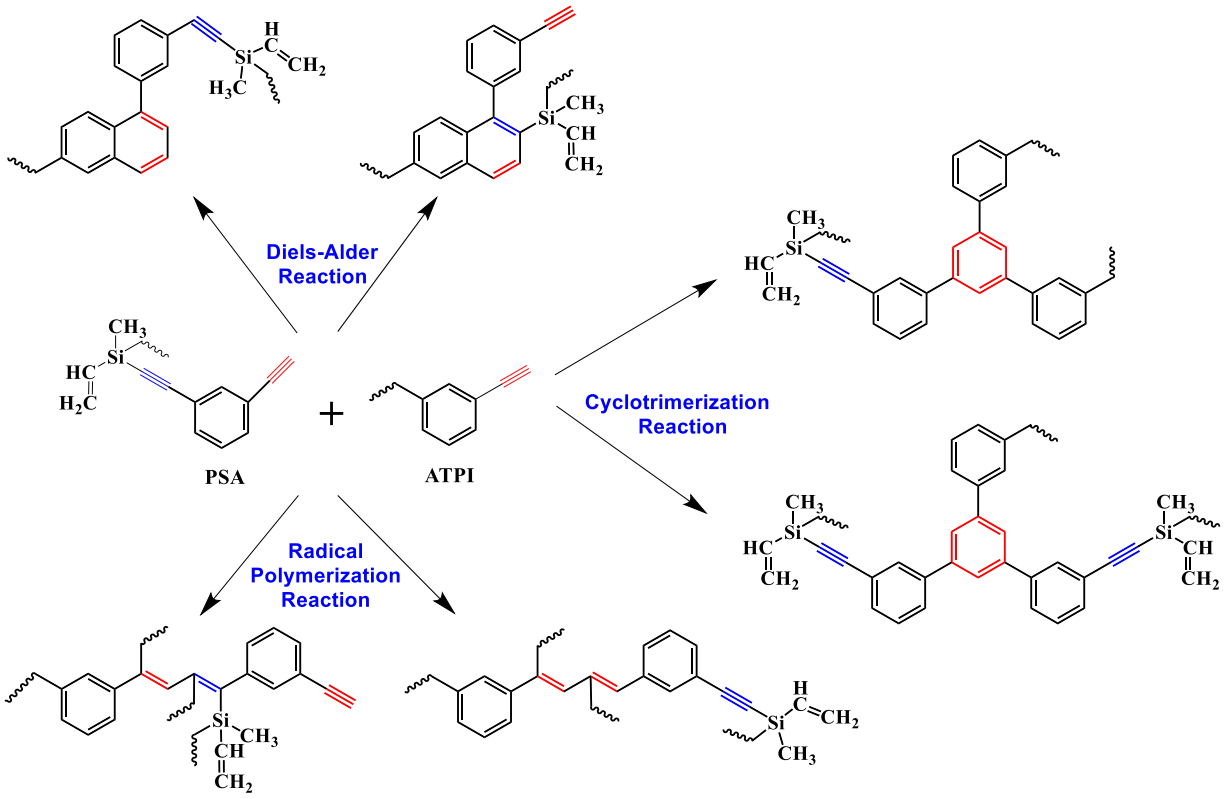

Figure 4. Copolymerization reaction between PSA and ATPI during the curing process.

The molecular structure of the PSA and the copolymerization reaction process are schematically illustrated in Figure 4.

The flexural properties of the blend resins with various contents of ATPI were first characterized to gain insight into the toughness of resins. The result is shown in Figure 5 (for details, see Table 1), where the effect of the prepolymerization temperature is also included. As shown, when the ATPI content increases, the flexural strength of the blend resins first increases and then decreases. The flexural strength increases slightly as the ATPI content is smaller than ca. 20 wt % but increases much as the ATPI content reaches ca. 30 wt %. The result implies that the addition of ATPI can improve the toughness of PSA resins. The improvement of toughness can be attributed to the copolymerization between PSA and ATPI. The alkynyl groups in both PSA and ATPI are first subjected to a reaction in DMF solution in the prepolymerization process and then subjected to an adequate reaction during curing. The ATPI and PSA molecules could form interpenetrating networks because of copolymerization. In addition to the inherent toughness of ATPI, the addition of ATPI molecules can relatively reduce the cross-linking density between the alkynyl groups of PSA resins and, therefore, improve the toughness of the cured PSA resins. One can also see from Figure 5 that the prepolymerization temperature has a marked effect on the flexural strength of the blend resins. The flexural strength is maximized at the prepolymerization temperature of 160 °C, as compared to that at 150 and 170 °C. In particular, the flexural strength of the resins with ATPI content of 30 wt % reaches 54.36 MPa, which is ca. 164% larger than that of pure PSA at the prepolymerization temperature of 160 °C.

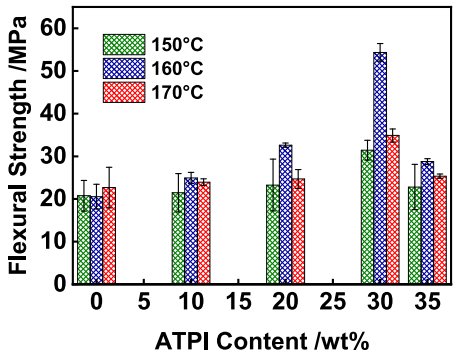

Figure 5. Flexural strength as a function of the ATPI content for PSA/ATPI resins prepolymerized at various temperatures. Three colors represent the three temperatures at which the PSA/ATPI resins are prepolymerized.

Table 1. Flexural Strength of the PSA/ATPI Blend Resin Prepolymerized at Various Temperatures

	flexural strength[a] (MPa)		
sample	150 °C	160 °C	170 °C
0 wt % ATPI (PSA)	20.76 ± 3.59	20.55 ± 2.90	22.67 ± 4.75
10 wt % ATPI	21.46 ± 4.48	25.00 ± 1.28	23.90 ± 0.78
20 wt % ATPI	23.27 ± 6.05	32.63 ± 0.50	24.69 ± 2.21
30 wt % ATPI	33.11 ± 2.33	54.36 ± 2.07	37.06 ± 1.53
35 wt % ATPI	22.81 ± 5.31	28.79 ± 0.69	25.34 ± 0.50

[a]The flexural strength of all samples was obtained by an electronic universal testing machine, and the specimens with dimensions of 80 × 15 × 4 mm were tested in a three-point loading mode.

We then analyzed the fracture surface morphologies of the cured PSA/ATPI resins prepolymerized at the temperature of 160 °C via SEM characterization. Figure 6 shows the SEM images for the cured PSA/ATPI resins with various ATPI

https://dx.doi.org/10.1021/acsami.0c06292
ACS Appl. Mater. Interfaces 2020, 12, 27587−27597

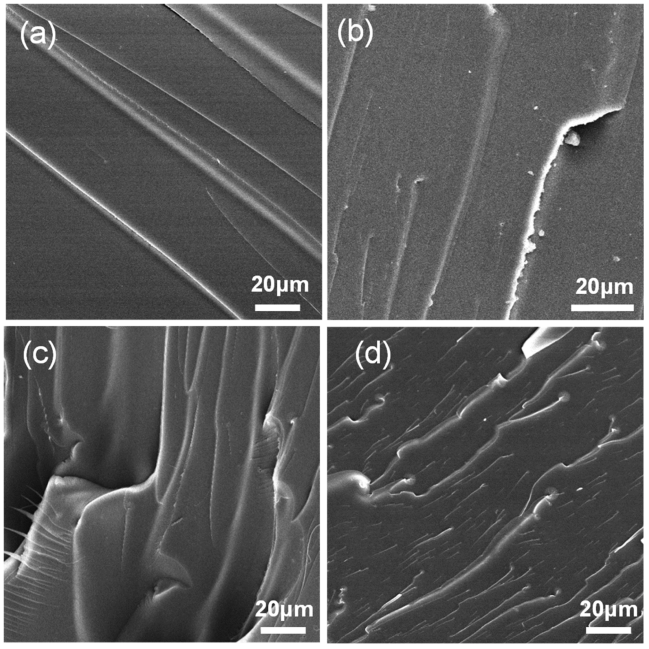

Figure 6. SEM images of the fracture surface of the cured PSA/ATPI resins with ATPI contents of (a) 0 wt % (neat PSA), (b) 20 wt %, (c) 30 wt %, and (d) 35 wt %. The resin was prepolymerized at a temperature of 160 °C.

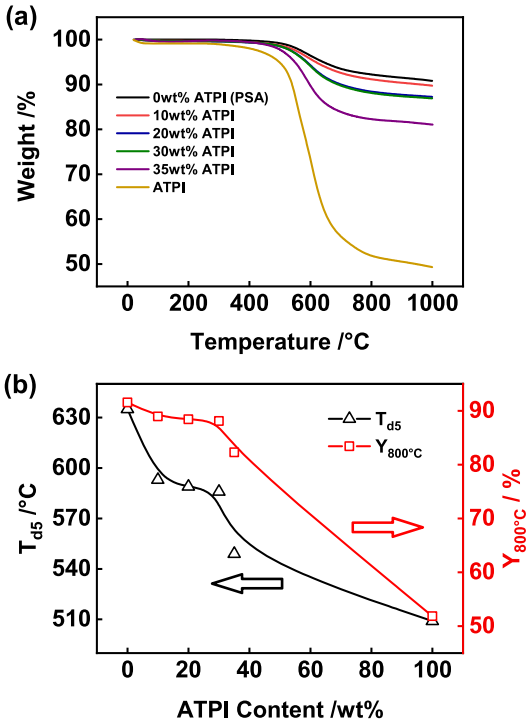

Figure 7. (a) TGA curves for the cured PSA/ATPI resins with various ATPI contents. (b) T_{d5} and $Y_{800°C}$ of cured PSA/ATPI resins as a function of ATPI contents. The resin is prepolymerized at a temperature of 160 °C.

contents. As shown in Figure 6a, the fractured surface of pure PSA thermosets exhibits a smooth and straight fracture line with no trace of plastic deformation. After the addition of ATPI, we did not observe any apparent phase separation phenomenon on the fracture surface of the cured PSA/ATPI resins (see Figure 6b–d), which indicates that the PSA has excellent compatibility with the ATPI. Meanwhile, the twisted fracture lines and grooves appear on the fracture surfaces. The groove depth increases first and then decreases with the increase of ATPI content, where the deepest groove appears at the ATPI content of 30 wt %. The results of the fracture surface morphologies are in agreement with the flexural properties. The change of fracture surface morphology indicates the addition of ATPI leads to plastic deformation of cured PSA/ATPI resins before fracture and improving the toughness of pure PSA.

To see the thermal stability, we carried out a TGA measurement for the cured PSA/ATPI resins under a nitrogen atmosphere at the heating rate of 10 °C/min. The obtained TGA curves are shown in Figure 7a. The decomposition temperature at 5% weight loss (T_{d5}) and the char yield at 800 °C ($Y_{800°C}$) obtained from the curve are shown in Figure 7b. The result showed that the PSA thermosets exhibit excellent thermal stability, where the T_{d5} is 635 °C and the $Y_{800°C}$ is 91.56 wt %. The ATPI thermosets, with T_{d5} of 509 °C and $Y_{800°C}$ of 52 wt %, also exhibit excellent thermal stability. Both the T_{d5} and the $Y_{800°C}$ of the blend thermosets decrease slightly with the increase of ATPI contents from 10 to 30 wt %. Such a slight decrease is acceptable. For example, the T_{d5} of the blend resins can maintain up to 586 °C as the content of ATPI is 30 wt %. As the ATPI content reaches 35 wt %, the T_{d5} and the $Y_{800°C}$ decrease to 549 °C and 82.28%, respectively. Because of the significant improvement in flexural performance and a slight decrease in thermal stability, the blend resins could well meet the performance requirements of advanced high-temperature-resistant polymer composites.

In addition to the toughness and heat resistance, the processability of the PSA/ATPI resins is also critical for material preparation. We, therefore, examined the rheological properties of PSA/ATPI resins with various ATPI contents prepolymerized at 160 °C, as shown in Figure 8. It can be seen

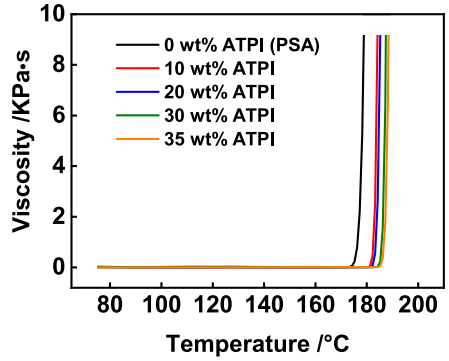

Figure 8. Plots of the viscosity as a function of the temperature for the PSA/ATPI resins prepolymerized at 160 °C. The sudden increase of viscosity indicates that the PSA/ATPI resins begin to gelatinize.

that the processing window of PSA/ATPI broadens with the increase of ATPI content, which is mainly caused by the decrease in the number density of alkynyl groups in the blends. (Note that the polyimide molecular chain contains only the outer alkynyl group.) Compared to the pure PSA, the number density of alkynyl groups of PSA/ATPI decreases with the increase of the polyimide content, which further leads to an increase in the gelation time of the blend resin. Also, it should

https://dx.doi.org/10.1021/acsami.0c06292
ACS Appl. Mater. Interfaces 2020, 12, 27587−27597

be noted that the ATPI cannot be cast because its melting point is higher than the temperature at which the terminal acetylene group starts to react. Compared to pure ATPI, the addition of PSA improves the processability greatly.

3.3. Toughening Mechanism of Blend Resin at Different Prepolymerization Temperatures. Of interest is that the flexural strength is maximized at the prepolymerization temperature of 160 °C, as compared to those at 150 and 170 °C. The prepolymerization temperatures play an important role in determining the flexural properties of the cured resins because the microstructure of the blend resin is greatly affected by the prepolymerization process. For the PSA/ATPI resins, the curing reaction degree of PSA/ATPI resins and the compatibility between PSA and ATPI have a significant influence on properties. The interplay of these two factors plays an essential role in determining the flexural strength.[44]

To gain insight into the effect of prepolymerization temperature on the reaction degree of PSA/ATPI resins, we first examined the rheological behavior of the PSA/ATPI resins with 30 wt % ATPI. Figure 9a shows the viscosity of the PSA/ATPI resins as a function of curing time. As shown, the gelation times of the resins are 43, 26, and 11 min at 150, 160, and 170 °C, respectively. Note that the prepolymerization times for PSA/ATPI resins at different temperatures are the same (1 h); a fast curing speed can indicate a high cross-linking degree achieved in the prepolymerization. The result shows that the reaction degree of PSA/ATPI resin with 30 wt % ATPI increases with the increase of temperature within 1 h. We also tracked the curing behavior of the PSA/ATPI resins at various temperatures by *in situ* FTIR. The FTIR curves are shown in Figure 9b. The strength of the ≡C−H stretching vibration peak at 3254 cm^{-1} and C≡C stretching vibration peak at 2156 cm^{-1} decrease with the increase of temperature, indicating that the reaction degree of terminal acetenyl groups gradually increases with the increase of temperature. To observe the variation of stretching vibration peaks in FTIR curves more clearly, we analyzed the FTIR spectra and estimated the degree of curing (see section 9 of the Supporting Information). The result shows the degree of curing increases with the increase of temperature from 150 to 170 °C, which agrees with the finding of rheologic studies. Such an increase in the curing reaction degree causes a decrease in resin toughness.[45]

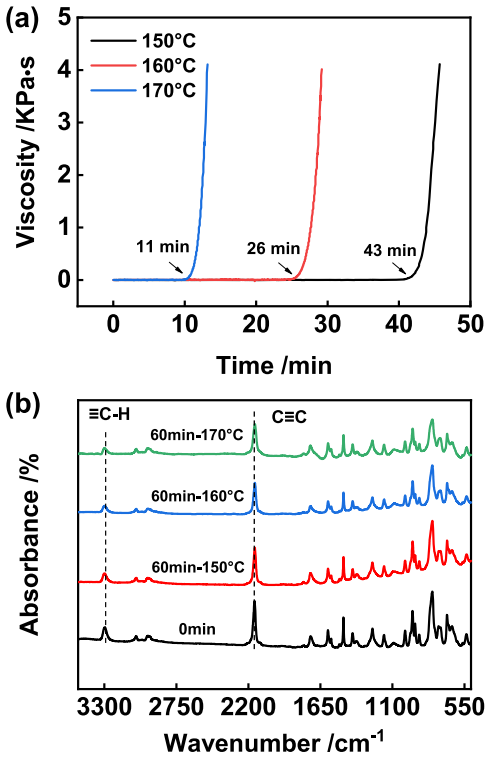

Figure 9. (a) Plots of the viscosity as a function of time for 30 wt % ATPI resin curing at various temperatures. (b) *In situ* FTIR curves for 30 wt % ATPI resin curing at various temperatures for 1 h.

Note that the reactions of the acetenyl groups can happen in three possible ways: (1) reaction between the acetenyl groups of PSA, (2) reaction between the acetenyl groups of ATPI, and (3) reaction between the acetenyl groups of ATPI and the acetenyl groups of PSA. Although the degree of the reaction between acetenyl groups increases as the temperature increases, it is still unclear which type of reactions occur at different prepolymerization temperatures. Studying the compatibility between PSA and ATPI can give information for the possible reaction way in the prepolymerization.

Because it is challenging to gain insight into the compatibility between PSA and ATPI at the experimental level, we applied the molecular dynamics (MD) simulation method to explore the phase behavior of the PSA/ATPI resin with 30 wt % ATPI. The MD simulation is a robust method for studying the phase behavior of the resins.[35] One can obtain the microstructure through the MD simulation. A representative microstructure of the blend resin is shown in Figure 10a. As shown, it is hard to gain insight into the compatibility between ATPI and PSA directly from this snapshot. Therefore, we used radial distribution functions $g(r)$ to characterize the MD results to understand how the ATPI and PSA mix in the prepolymerization solution. The $g(r)$ represents the probability of finding a molecule at distance r (see the upper-right corner of Figure 10a). A broader distribution with $g(r) \approx 1$ implies a more homogeneous and disordered mix of the alkynyl groups.[46]

Figure 10b shows the radial distribution function $g(r)$ between the alkynyl groups of PSA and ATPI in the blend resin solution at various temperatures. In the figure, the abscissa and ordinate represent the distance r between the alkynyl groups of two molecules and the probability of finding the alkynyl groups of the molecules at the distance r, respectively. As shown in Figure 10b, the $g(r)$ has a value of around 1.0, which implies that the ATPI and PSA mix well in DMF at these temperatures. With the increase of temperatures, the $g(r)$ decays to a constant value of 1 more quickly, which indicates that the PSA and ATPI mix better at a higher temperature. The increase in disorder of the blend can increase the contact/reaction probability between the alkynyl groups of PSA and ATPI and, therefore, the toughness of the thermosets.

The interplay of the compatibility and curing reaction degree determines the final properties of the thermosets. On the one hand, the curing reaction degree increases with the increase of prepolymerization temperature (see Figure 9), which causes a decrease of toughness. On the other hand, the PSA and ATPI mix better with increasing prepolymerization temperature, which can help to increase the toughness. We, therefore, deduced that the toughness could be maximized at an intermediate temperature where the PSA and ATPI are sufficiently reacted yet the curing degree is not too high.

https://dx.doi.org/10.1021/acsami.0c06292
ACS Appl. Mater. Interfaces 2020, 12, 27587−27597

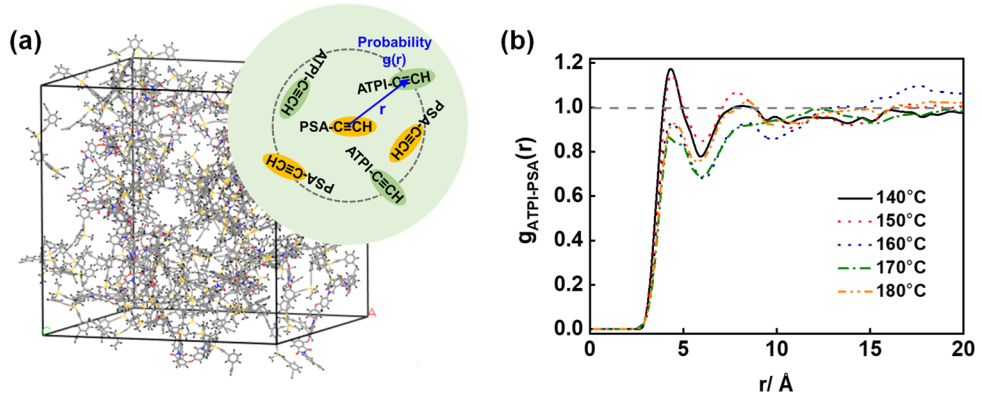

Figure 10. (a) Microstructure of the blend resin solution obtained at 140 °C for MD simulation of 200 ps. The upper-right corner shows a schematic of the radial distribution function $g_{ATPI-PSA}(r)$. (b) Radial distribution function $g_{ATPI-PSA}(r)$ between the alkynyl groups of PSA and the alkynyl groups of ATPI in the resin solution at various temperatures. The resin solution contains 12.4 wt % ATPI, 29.0 wt % PSA, and 58.6 wt % DMF.

Namely, the balance of cross-linking degree and mixing degree results in the optimized flexural strength at an intermediate prepolymerization temperature (160 °C in the present work).

To observe the superiority of the blend resins, we compared the thermal and flexural properties of our resins with those of other resins (the data were collected from the literature listed in section 10 of the Supporting Information). Figure 11 shows

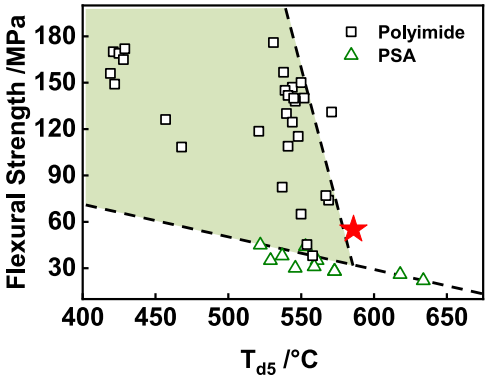

Figure 11. Flexural strength versus 5% thermal decomposition temperature (T_{d5}) for existing tough resins. The black squares and the green triangles correspond to polyimide resins and silicon-containing arylacetylene resins, respectively. The data were collected from the literature listed in section 10 of the Supporting Information. The red star represents PSA/ATPI blend resins with 30 wt % ATPI.

the plot of flexural properties against thermal properties. One can see that the polyimide resins are located in the area of the low decomposition temperature and high toughness, whereas the silicon-containing arylacetylene resins are located in the area of the high decomposition temperature and low toughness. In contrast, our blend resin is beyond these two regimes, which has excellent combined properties of the high decomposition temperature and high toughness.

The present work reports for the first time that MGA is established for designing and screening acetylene-terminated polyimides. We found that the PSA/ATPI resins toughened with ATPI have excellent combined properties, that is, higher toughness than pure PSA and higher thermal stability and easier processability than pure ATPI. The present study presents a method for accelerating the development of heat-resistant thermosets with high toughness, which could expand to the exploration and exploitation of other advanced polymer materials.

4. CONCLUSIONS

A materials genome approach (MGA) was established to screen acetylene-terminated polyimides that are used for improving the toughness of heat-resistant PSA resins. An acetylene-terminated polyimide, named ATPI, was filtered out by using the developed MGA and was synthesized to blend with PSA resins. The effect of ATPI content and prepolymerization temperature on the properties of the blend resins was investigated. It was found that the blend resins with 30% ATPI exhibit excellent toughness and high-temperature resistance as the resins are prepolymerized at the temperature of 160 °C. The combination of experimental results and MD simulations revealed that the balance of cross-linking degree and mixing degree determines the optimized flexural strength. The present work provides a method combining theoretical prediction and experimental preparation to accelerate the exploration of advanced polymeric materials.

■ ASSOCIATED CONTENT

Supporting Information

The Supporting Information is available free of charge at https://pubs.acs.org/doi/10.1021/acsami.0c06292.

Full details include the molecular dynamics simulation, the experimental method, the molecules of dianhydrides and diamines used for gene combinations, a list of the literature where the data for Figure 2 are obtained, the verification of MGA results, characterizations of ATPI molecules, the solubility of ATPI, the chemical structure of the cured resin and thermal curing mechanism, the degree of curing of the PSA/ATPI resins, and a list of the literature where the data for Figure 11 are obtained (PDF)

■ AUTHOR INFORMATION

Corresponding Authors

Liquan Wang − *Shanghai Key Laboratory of Advanced Polymeric Materials, Key Laboratory for Ultrafine Materials of Ministry of Education, School of Materials Science and Engineering, East China University of Science and Technology,*

https://dx.doi.org/10.1021/acsami.0c06292
ACS Appl. Mater. Interfaces 2020, 12, 27587−27597

Shanghai 200237, China; orcid.org/0000-0002-5141-8584; Email: lq_wang@ecust.edu.cn

Jiaping Lin − *Shanghai Key Laboratory of Advanced Polymeric Materials, Key Laboratory for Ultrafine Materials of Ministry of Education, School of Materials Science and Engineering, East China University of Science and Technology, Shanghai 200237, China;* orcid.org/0000-0001-9633-4483; Email: jlin@ecust.edu.cn

Authors

Guanru Gao − *Shanghai Key Laboratory of Advanced Polymeric Materials, Key Laboratory for Ultrafine Materials of Ministry of Education, School of Materials Science and Engineering, East China University of Science and Technology, Shanghai 200237, China*

Songqi Zhang − *Shanghai Key Laboratory of Advanced Polymeric Materials, Key Laboratory for Ultrafine Materials of Ministry of Education, School of Materials Science and Engineering, East China University of Science and Technology, Shanghai 200237, China*

Huimin Qi − *Shanghai Key Laboratory of Advanced Polymeric Materials, Key Laboratory for Ultrafine Materials of Ministry of Education, School of Materials Science and Engineering, East China University of Science and Technology, Shanghai 200237, China;* orcid.org/0000-0003-4742-2561

Junli Zhu − *Shanghai Key Laboratory of Advanced Polymeric Materials, Key Laboratory for Ultrafine Materials of Ministry of Education, School of Materials Science and Engineering, East China University of Science and Technology, Shanghai 200237, China*

Lei Du − *Shanghai Key Laboratory of Advanced Polymeric Materials, Key Laboratory for Ultrafine Materials of Ministry of Education, School of Materials Science and Engineering, East China University of Science and Technology, Shanghai 200237, China*

Ming Chu − *Shanghai Key Laboratory of Advanced Polymeric Materials, Key Laboratory for Ultrafine Materials of Ministry of Education, School of Materials Science and Engineering, East China University of Science and Technology, Shanghai 200237, China*

Complete contact information is available at: https://pubs.acs.org/10.1021/acsami.0c06292

Author Contributions

[#]G.G. and S.Z. contributed equally to this work.

Notes

The authors declare no competing financial interest.

■ ACKNOWLEDGMENTS

This work was supported by the National Natural Science Foundation of China (51833003, 21774032, 51621002, and 21975073).

■ REFERENCES

(1) Itoh, M.; Iwata, K.; Ishikawa, J.-I.; Sukawa, H.; Kimura, H.; Okita, K. Various Silicon-Containing Polymers with Si(H)-C≡C Units. *J. Polym. Sci., Part A: Polym. Chem.* **2001**, *39*, 2658−2669.

(2) Wang, M.; Ning, Y. Oligosilylarylnitrile: The Thermoresistant Thermosetting Resin with High Comprehensive Properties. *ACS Appl. Mater. Interfaces* **2018**, *10*, 11933−11940.

(3) Chen, M.; Liu, Y.; Lin, J.; Liu, C. Characterization of a Novel Silicon-Containing Hybrid Polymer by Thermal Curing, Pyrolysis Behavior, and Fluorescence Analysis. *J. Appl. Polym. Sci.* **2019**, *136*, 47403.

(4) Barile, C.; Casavola, C.; De Cillis, F. Mechanical Comparison of New Composite Materials for Aerospace Applications. *Composites, Part B* **2019**, *162*, 122−128.

(5) Itoh, M.; Mitsuzuka, M.; Iwata, K.; Inoue, K. A Novel Synthesis and Extremely High Thermal Stability of Poly[(phenylsilylene)-ethynylene-1,3-phenyleneethynylene]. *Macromolecules* **1994**, *27*, 7917−7919.

(6) Huang, J.; Du, W.; Zhang, J.; Huang, F.; Du, L. Study on the Copolymers of Silicon-Containing Arylacetylene Resin and Acetylene-Functional Benzoxazine. *Polym. Bull.* **2009**, *62*, 127−138.

(7) Li, Q.; Zhou, Y.; Hang, X.; Deng, S.; Huang, F.; Du, L.; Li, Z. Synthesis and Characterization of a Novel Arylacetylene Oligomer Containing POSS Units in Main Chains. *Eur. Polym. J.* **2008**, *44*, 2538−2544.

(8) Zhang, J.; Huang, J.; Yu, X.; Wang, C.; Huang, F.; Du, L. Preparation and Properties of Modified Silicon-Containing Arylacetylene Resin with Bispropargyl Ether. *Bull. Korean Chem. Soc.* **2012**, *33*, 3706−3710.

(9) Gao, Y.; Zhou, Y.; Huang, F.; Du, L. Preparation and Properties of Silicon-Containing Arylacetylene Resin/Benzoxazines Blends. *High Perform. Polym.* **2013**, *25*, 445−453.

(10) Cella, J. A. Degradation and Stability of Polyimides. *Polym. Degrad. Stab.* **1992**, *36*, 99−110.

(11) Elmehalmey, W. A.; Azzam, R. A.; Hassan, Y. S.; Alkordi, M. H.; Madkour, T. M. Imide-Based Polymers of Intrinsic Microporosity: Probing the Microstructure in Relation to CO_2 Sorption Characteristics. *ACS Omega* **2018**, *3*, 2757−2764.

(12) Liaw, D.; Wang, K.; Huang, Y.; Lee, K.; Lai, J.; Ha, C. Advanced Polyimide Materials: Syntheses, Physical Properties and Applications. *Prog. Polym. Sci.* **2012**, *37*, 907−974.

(13) Kanehashi, S.; Onda, M.; Shindo, R.; Sato, S.; Kazama, S.; Nagai, K. Synthesis, Characterization, and CO_2 Permeation Properties of Acetylene-Terminated Polyimide Membranes. *Polym. Eng. Sci.* **2013**, *53*, 1667−1675.

(14) Cho, D.; Drzal, L. T. Phenylethynyl-Terminated Polyimide, Exfoliated Graphite Nanoplatelets, and the Composites: An Overview. *Carbon Lett.* **2016**, *19*, 1−11.

(15) Pickard, J.; Jones, E.; Goldfarb, I. Kinetics and Mechanism of the Bulk Thermal Polymerization of (3-phenoxyphenyl)acetylene. *Macromolecules* **1979**, *12*, 895−902.

(16) Guo, K.; Li, P.; Zhu, Y.; Wang, F.; Qi, H. Thermal Curing and Degradation Behaviour of Silicon-Containing Arylacetylene Resins. *Polym. Degrad. Stab.* **2016**, *131*, 98−105.

(17) Swanson, S.; Fleming, W.; Hofer, D. Acetylene-Terminated Polyimide Cure Studies Using Carbon-13 Magic-Angle Spinning NMR on Isotopically Labeled Samples. *Macromolecules* **1992**, *25*, 582−588.

(18) Tenney, D. R.; Davis, J. G., Jr.; Johnston, N. J.; Pipes, R. B.; McGuire, J. F. Structural Framework for Flight I: NASA's Role in Development of Advanced Composite Materials for Aircraft and Space Structures. NASA/CR-2019-220267. 2019.

(19) Lu, X. Remarks on the Recent Progress of Materials Genome Initiative. *Sci. Bull.* **2015**, *60*, 1966−1968.

(20) Raccuglia, P.; Elbert, K. C.; Adler, P. D.; Falk, C.; Wenny, M. B.; Mollo, A.; Zeller, M.; Friedler, S. A.; Schrier, J.; Norquist, A. J. Machine-Learning-Assisted Materials Discovery Using Failed Experiments. *Nature* **2016**, *533*, 73−76.

(21) Warren, J. A. The Materials Genome Initiative and Artificial Intelligence. *MRS Bull.* **2018**, *43*, 452−457.

(22) Liu, Y.; Hu, Z.; Suo, Z.; Hu, L.; Feng, L.; Gong, X.; Liu, Y.; Zhang, J. High-Throughput Experiments Facilitate Materials Innovation: A Review. *Sci. China: Technol. Sci.* **2019**, *62*, 521−545.

(23) Kalidindi, S. R.; Brough, D. B.; Li, S.; Cecen, A.; Blekh, A. L.; Congo, F. Y. P.; Campbell, C. Role of Materials Data Science and Informatics in Accelerated Materials Innovation. *MRS Bull.* **2016**, *41*, 596−602.

(24) Wang, Y.; Liu, Y.; Song, S.; Yang, Z.; Qi, X.; Wang, K.; Liu, Y.; Zhang, Q.; Tian, Y. Accelerating the Discovery of Insensitive High-Energy-Density Materials by a Materials Genome Approach. *Nat. Commun.* **2018**, *9*, 2444.
(25) Gautier, R.; Zhang, X.; Hu, L.; Yu, L.; Lin, Y.; Sunde, T. O.; Chon, D.; Poeppelmeier, K. R.; Zunger, A. Prediction and Accelerated Laboratory Discovery of Previously Unknown 18-Electron ABX Compounds. *Nat. Chem.* **2015**, *7*, 308−316.
(26) Boyd, P. G.; Lee, Y.; Smit, B. Computational Development of the Nanoporous Materials Genome. *Nat. Rev. Mater.* **2017**, *2*, 17037.
(27) Li, Y.; Cao, H.; Yu, J. Toward a New Era of Designed Synthesis of Nanoporous Zeolitic Materials. *ACS Nano* **2018**, *12*, 4096−4104.
(28) Lorenzini, R. G.; Kline, W. M.; Wang, C.; Ramprasad, R.; Sotzing, G. The Rational Design of Polyurea & Polyurethane Dielectric Materials. *Polymer* **2013**, *54*, 3529−3533.
(29) Sharma, V.; Wang, C.; Lorenzini, R.; Ma, R.; Zhu, Q.; Sinkovits, D.; Pilania, G.; Oganov, A.; Kumar, S.; Sotzing, G.; Boggs, S.; Ramprasad, R. Rational Design of All Organic Polymer Dielectrics. *Nat. Commun.* **2014**, *5*, 4845.
(30) Huan, T.; Mannodi-Kanakkithodi, A.; Kim, C.; Sharma, V.; Pilania, G.; Ramprasad, R. A Polymer Dataset for Accelerated Property Prediction and Design. *Sci. Data* **2016**, *3*, 160012.
(31) Mannodi-Kanakkithodi, A.; Treich, G.; Huan, T.; Ma, R.; Tefferi, M.; Cao, Y.; Sotzing, G.; Ramprasad, R. Rational Co-Design of Polymer Dielectrics for Energy Storage. *Adv. Mater.* **2016**, *28*, 6277−6291.
(32) Mannodi-Kanakkithodi, A.; Chandrasekaran, A.; Kim, C.; Huan, T.; Pilania, G.; Botu, V.; Ramprasad, R. Scoping the Polymer Genome: A Roadmap for Rational Polymer Dielectrics Design and Beyond. *Mater. Today* **2018**, *21*, 785−796.
(33) Bicerano, J. *Prediction of Polymer Properties*; CRC Press: 2002.
(34) Lu, Y.; Shu, Y.; Liu, N.; Shu, Y.; Wang, K.; Wu, Z.; Wang, X.; Ding, X. Theoretical Simulations on the Glass Transition Temperatures and Mechanical Properties of Modified Glycidyl Azide Polymer. *Comput. Mater. Sci.* **2017**, *139*, 132−139.
(35) Xu, Z.; Lin, J.; Zhang, Q.; Wang, L.; Tian, X. Theoretical Simulations of Nanostructures Self-Assembled from Copolymer Systems. *Polym. Chem.* **2016**, *7*, 3783−3811.
(36) Xu, P.; Lin, J.; Zhang, L. Distinct Viscoelasticity of Nanoparticle-Tethering Polymers Revealed by Nonequilibrium Molecular Dynamics Simulations. *J. Phys. Chem. C* **2017**, *121*, 28194−28203.
(37) Zhang, Q.; Lin, J.; Wang, L.; Xu, Z. Theoretical Modeling and Simulations of Self-Assembly of Copolymers in Solution. *Prog. Polym. Sci.* **2017**, *75*, 1−30.
(38) BIOVIA Materials Studio. https://www.3dsbiovia.com/products/collaborative-science/biovia-materials-studio/ (accessed May 24, 2020).
(39) He, Y.; Zhou, Y.; Xi, Q.; Cui, H.; Luo, T.; Song, H.; Nie, X.; Wang, L.; Ying, B. Genetic Variations in Microrna Processing Genes Are Associated with Susceptibility in Depression. *DNA Cell Biol.* **2012**, *31*, 1499−1506.
(40) PoLyInfo Database: https://polymer.nims.go.jp/index_en.html (accessed May 24, 2020).
(41) Polymer Genome: www.polymergenome.org (accessed May 24, 2020).
(42) Kim, C.; Chandrasekaran, A.; Huan, T. D.; Das, D.; Ramprasad, R. Polymer Genome: A Data-Powered Polymer Informatics Platform for Property Predictions. *J. Phys. Chem. C* **2018**, *122*, 17575−17585.
(43) Chen, Z.; Wang, L.; Lin, J.; Du, L. Theoretical Study on Thermal Curing Mechanism of Arylethynyl-Containing Resins. *Phys. Chem. Chem. Phys.* **2020**, *22*, 6468−6477.
(44) Salmoria, G.; Ahrens, C.; Fredel, M.; Soldi, V.; Pires, A. T. N. Stereolithography Somos 7110 Resin: Mechanical Behavior and Fractography of Parts Post-Cured by Different Methods. *Polym. Test.* **2005**, *24*, 157−162.
(45) Singh, R.; Zhang, M.; Chan, D. Toughening of a Brittle Thermosetting Polymer: Effects of Reinforcement Particle Size and Volume Fraction. *J. Mater. Sci.* **2002**, *37*, 781−788.
(46) Bermejo, J. S.; Ugarte, C. M. Influence of Cross-Linking Density on the Glass Transition and Structure of Chemically Cross-Linked PVA: A Molecular Dynamics Study. *Macromol. Theory Simul.* **2009**, *18*, 317−327.

https://dx.doi.org/10.1021/acsami.0c06292
ACS Appl. Mater. Interfaces 2020, 12, 27587−27597